

Article

# IAM Chromatographic Models of Skin Permeation

Anna W. Sobańska \*  and Elżbieta Brzezińska

Department of Analytical Chemistry, Faculty of Pharmacy, Medical University of Lodz, ul. Muszyńskiego 1, 90-151 Lodz, Poland; elzbieta.brzezinska@umed.lodz.pl

\* Correspondence: anna.sobanska@umed.lodz.pl

**Abstract:** Chromatographic retention factor  $\log k_{IAM}$  obtained from IAM HPLC chromatography with buffered aqueous mobile phases and calculated molecular descriptors (surface area— $S_a$ ; molar volume— $V_M$ ; polar surface area— $PSA$ ; count of freely rotatable bonds— $FRB$ ; H-bond acceptor count— $HA$ ; energy of the highest occupied molecular orbital— $E_{HOMO}$ ; energy of the lowest unoccupied orbital— $E_{LUMO}$ ; and polarizability— $\alpha$ ) obtained for a group of 160 structurally unrelated compounds were tested in order to generate useful models of solutes' skin permeability coefficient  $\log K_p$ . It was established that  $\log k_{IAM}$  obtained in the conditions described in this study is not sufficient as a sole predictor of the skin permeability coefficient. Simple put, potentially useful models based on  $\log k_{IAM}$  and readily available calculated descriptors, accounting for 85 to 91% of the total variability, were generated using Multiple Linear Regression (MLR). The models proposed in the study were tested on a group of 20 compounds with known experimental  $\log K_p$  values.

**Keywords:** Immobilized Artificial Membrane; HPLC; calculated descriptors; skin permeation



**Citation:** Sobańska, A.W.; Brzezińska, E. IAM Chromatographic Models of Skin Permeation. *Molecules* **2022**, *27*, 1893. <https://doi.org/10.3390/molecules27061893>

Academic Editor: Angelo Antonio D'Archivio

Received: 17 February 2022

Accepted: 12 March 2022

Published: 15 March 2022

**Publisher's Note:** MDPI stays neutral with regard to jurisdictional claims in published maps and institutional affiliations.



**Copyright:** © 2022 by the authors. Licensee MDPI, Basel, Switzerland. This article is an open access article distributed under the terms and conditions of the Creative Commons Attribution (CC BY) license (<https://creativecommons.org/licenses/by/4.0/>).

## 1. Introduction

Transepidermal absorption is an important route of chemicals' entry into a human body. The skin permeability coefficient  $K_p$  is defined according to Equation (1):

$$K_p = \frac{K_m D}{h} \quad (1)$$

where  $K_m$  is the partition coefficient between the stratum corneum and the vehicle;  $D$  is the effective compound's diffusion coefficient through the stratum corneum; and  $h$  is the diffusional pathlength.

The experimental values of skin permeability coefficients obtained in vivo (on human volunteers), ex vivo (on excised human skin), or even on animal models [1] are scarce and often inconsistent due to variations in properties of different skin specimen; there are also some ethical considerations related to such models. For these reasons, several in vitro or in silico skin permeation models have been developed [2]. One of the most frequently cited in silico skin permeability models, based on just two descriptors known to have a very strong influence on compounds' ability to cross biological barriers, namely lipophilicity (expressed as octanol-water partition coefficient  $K_{ow}$ ) and molecular weight ( $M_w$ ), has been proposed by Potts (Equation (2)) [3]:

$$\log K_p = -2.80 + 0.66 \log K_{ow} - 0.0056 M_w \quad (2)$$

The Potts model is widely acknowledged due to its simplicity [4], although it is criticized by some research studies because it gives erroneous results for compounds of extreme properties (very hydrophilic or lipophilic; non-hydrogen bonding or very strongly hydrogen-bonding) [5–8]. However, the predictions made using Pott's model are sufficiently good for the majority of drug-like compounds [9,10], thus this model is a popular tool in drugs' ADMET studies and calculations based on it are offered by some

popular ADMET prediction software packages [11,12]. Other proposed theoretical  $K_p$  models are based on the descriptors, such as the melting point, McGowan's characteristic volume, Abraham's solvation parameters or H-bonding properties (total H-bond count, H-bond acceptor count, and H-bond donor count), and total nitrogen and oxygen atom count [13–23]. QSAR studies of skin permeation published to date prove that transdermal absorption is a complex property and there are several factors contributing to it [4,7,24–29].

Previous studies demonstrated the usefulness of chromatographic descriptors in skin permeability studies. Liquid chromatographic models of skin permeability are based on the notion that the solutes' partition between a stationary phase and a mobile phase resembles the partition between the skin and the vehicle. The separation techniques capable of providing chromatographic skin permeability predictors are liquid chromatography (HPLC or TLC), biopartitioning micellar chromatography, micellar electrokinetic chromatography, liposome electrokinetic chromatography, and two-dimensional gas chromatography (GCxGC) [8,30–40]. Chromatographic techniques of skin permeability studies are growing in popularity because of their high throughput, low cost, and good repeatability/reproducibility (the majority of such studies are conducted on commercially available stationary phases).

In our earlier studies, we proposed models of  $K_p$  based on calculated molecular parameters and RP-18 TLC-derived descriptors ( $R_M$  or  $R_M/V_M$ ) [23,41]:

$$\log K_p = -1.66 (\pm 0.24) - 0.011 (\pm 0.005) PSA + 0.24 (\pm 0.05) HD - 0.0036 (\pm 0.0017) V_M + 2.01 (\pm 0.24) R_M \quad (3)$$

(steroids,  $n = 16$ ,  $R^2 = 0.99$ ,  $R^2_{adj.} = 0.98$ ,  $F = 229.0$ ,  $p < 0.01$ ,  $s_e = 0.18$ )

$$\log K_p = -1.65 (\pm 0.90) - 0.37 (\pm 0.03) (N+O) + 0.13 (\pm 0.03) \log D + 90.4 (\pm 43.0) (R_M/V_M) - 0.0000058 (\pm 0.0000019) E_T + 0.029 (\pm 0.01) E_h \quad (4)$$

(structurally diverse compounds,  $n = 60$ ,  $R^2 = 0.87$ ,  $R^2_{adj.} = 0.85$ ,  $F = 70.9$ ,  $p < 0.01$ ,  $s_e = 0.40$ )

where  $R_M = \log(1/R_f - 1)$  [42] and  $R_f$  values were collected on the RP-18 stationary phase with acetonitrile/pH 7.4 phosphate-buffered saline 70:30 ( $v/v$ ) as a mobile phase;  $\log D$  is the distribution coefficient;  $PSA$  is the polar surface area ( $\text{\AA}^2$ );  $HD$  is the H-bond donors count;  $V_M$  is the molar volume ( $\text{\AA}^3$ );  $E_T$  is the total energy (kcal/mol);  $E_h$  is the hydration energy (kcal/mol); and  $(N + O)$  is the total oxygen and nitrogen atom count.

We have also studied the skin permeability of organic sunscreens using RP-18 TLC-derived descriptors obtained with mobile phases containing different organic modifiers [43].

Thanks to the ability of stationary phases based on phosphatidylcholine covalently linked to aminopropyl silica to mimic the natural membrane bilayer (or, to be precise, a half of it), Immobilized Artificial Membrane (IAM) chromatography performed on such sorbents has been used to predict physico-chemical and biological properties of solutes for many years [44]. The relationships between the IAM chromatographic retention factor ( $k_{IAM}$ ) and the skin permeability coefficient have been studied for small groups of compounds ( $n = 10$  to 32) and the resulting dependencies are mostly univariate (linear or quadratic) [30,31,34,36], the exceptions being the study in which McGowan's characteristic volume  $V$  was incorporated in a model alongside with  $\log k_{IAM}$  [31]:

$$\log K_p = -3.58 + 2.56 \log k_{IAM} - 1.12 V \quad (5)$$

( $n = 32$ ,  $R^2 = 0.74$ )

Additionally, the model proposed by Barbato, based on a combination of an IAM chromatographic descriptor and the octanol-water partition coefficient  $\log K_{ow}$ , is as follows [30]:

$$\log K_p = -2.136 \Delta \log k_w^{IAM} + 0.037 \log K_{ow} - 2.373 \quad (6)$$

( $n = 10$ ,  $R^2 = 0.94$ )

where  $\Delta \log k_w^{IAM}$  is the difference between  $\log k_w^{IAM}$  measured and predicted on the basis of  $\log K_{ow}$ .

In this study it was our intention to investigate the potential of immobilized artificial membrane (IAM) chromatography in skin permeability studies of a large group of solutes from different chemical families. We hoped to provide simple and practical models based on the IAM chromatographic retention factors and calculated physico-chemical descriptors that could be used to predict the skin permeability coefficient of solutes by researchers both in drug discovery and environmental toxicology fields.

## 2. Results and Discussion

The experimentally determined values of  $K_p$  were available for only some drugs within the studied group. For this reason, the models of skin permeability involving IAM chromatographic and calculated descriptors were generated and validated using  $K_p$  values obtained in silico with the EpiSuite software (DERMWIN v. 2 module;  $\log K_p^{\text{EPI}}$ ), which is recommended by the US Environmental Protection Agency [12,45] and was tested on a sub-group of 20 solutes whose experimental  $\log K_p$  values are known ( $\log K_p^{\text{exp}}$ ) [29]. The estimation methodology used by DERMWIN was based on the above-mentioned Equation (2) [3]. The values of  $\log K_p^{\text{EPI}}$  obtained using DERMWIN are given in Table 1.

**Table 1.** IAM HPLC retention factors: reference, experimental, and calculated values of  $\log K_p$ .

No.	CAS No.		$\log k_{IAM}$	$\log K_p^{\text{EPI}}$	$\log K_p^{(9)}$	$\log K_p^{(11)}$	$\log K_p^{(12)}$	$\log K_p^{(13)}$	$\log K_p^{\text{exp}}$
<u>1</u>	103-84-4	acetanilide	0.48	-2.79	-2.91	-2.83	-2.92	-2.69	
<u>2</u>	98-86-2	acetophenone	0.76	-2.43	-2.42	-2.43	-2.55	-2.33	
<u>3</u>	95-55-6	2-aminophenol	0.28	-3.01	-2.97	-3.01	-2.89	-3.11	
<u>4</u>	100-66-3	anisole	1.06	-2.01	-2.08	-2.07	-2.19	-2.03	
<u>5</u>	100-52-7	benzaldehyde	0.63	-2.42	-2.52	-2.47	-2.58	-2.39	
<u>6</u>	55-21-0	benzamide	0.12	-3.06	-3.13	-3.14	-3.10	-3.13	
<u>7</u>	71-43-2	benzene	0.96	-1.83	-1.98	-1.95	-2.10	-1.91	
<u>8</u>	100-47-0	benzotrile	0.77	-2.35	-2.43	-2.41	-2.41	-2.45	
<u>9</u>	100-51-6	benzyl alcohol	0.35	-2.68	-2.58	-2.67	-2.77	-2.59	
<u>10</u>	92-52-4	biphenyl	2.88	-1.01	-1.01	-0.93	-1.03	-0.94	
<u>11</u>	90-11-9	1-bromonaphthalene	2.90	-1.27	-1.12	-0.92	-1.04	-0.93	
<u>12</u>	591-20-8	3-bromophenol	1.71	-2.03	-1.81	-1.75	-1.68	-1.91	
<u>13</u>	104-54-1	cinnamyl alcohol	1.02	-2.26	-2.43	-2.39	-2.52	-2.25	
<u>14</u>	91-64-5	coumarin	0.99	-2.70	-2.55	-2.40	-2.44	-2.38	
<u>15</u>	108-94-1	cyclohexanone	0.08	-2.82	-2.79	-2.80	-2.94	-2.67	
<u>16</u>	84-66-2	diethyl phthalate	1.63	-2.44	-2.37	-2.50	-2.39	-2.54	
<u>17</u>	576-26-1	2,6-dimethylphenol	1.25	-1.92	-2.11	-2.12	-2.15	-2.14	
<u>18</u>	623-05-2	4-hydroxybenzyl alcohol	0.12	-3.34	-3.10	-3.10	-3.08	-3.08	
<u>19</u>	95-48-7	2-methylphenol	1.02	-2.12	-2.21	-2.21	-2.23	-2.25	-1.80
<u>20</u>	106-44-5	4-methylphenol	1.02	-2.12	-2.21	-2.22	-2.23	-2.26	-1.76
<u>21</u>	91-20-3	naphthalene	2.47	-1.33	-1.25	-1.12	-1.22	-1.15	
<u>22</u>	90-15-3	1-naphthol	2.08	-1.72	-1.76	-1.64	-1.62	-1.72	
<u>23</u>	135-19-3	2-naphthol	1.93	-1.82	-1.88	-1.75	-1.76	-1.79	-1.55
<u>24</u>	88-74-4	2-nitroaniline	1.13	-2.35	-2.72	-2.70	-2.24	-3.16	
<u>25</u>	100-01-6	4-nitroaniline	1.01	-2.66	-2.78	-2.78	-2.35	-3.22	
<u>26</u>	98-95-3	nitrobenzene	1.04	-2.27	-2.49	-2.44	-2.20	-2.72	
<u>27</u>	619-73-8	4-nitrobenzyl alcohol	0.72	-2.83	-3.03	-2.98	-2.67	-3.26	
<u>28</u>	627-05-4	1-nitrobutane	0.42	-2.41	-2.70	-2.80	-2.59	-3.03	
<u>29</u>	99-99-0	4-nitrotoluene	1.35	-2.00	-2.34	-2.29	-2.05	-2.56	
<u>30</u>	108-95-2	phenol	0.68	-2.36	-2.38	-2.38	-2.40	-2.42	-2.09
<u>31</u>	60-12-8	2-phenylethanol	0.53	-2.59	-2.63	-2.65	-2.79	-2.50	
<u>32</u>	92-69-3	4-phenylphenol	2.56	-1.63	-1.44	-1.39	-1.37	-1.47	
<u>33</u>	108-88-3	toluene	1.40	-1.51	-1.71	-1.70	-1.83	-1.69	
<u>34</u>	106-48-9	4-chlorophenol	1.48	-1.94	-1.89	-1.87	-1.81	-2.02	-1.44
<u>35</u>	271-89-6	2,3-benzofuran	1.50	-1.69	-1.83	-1.85	-1.89	-1.88	
<u>36</u>	526-75-0	2,3-dimethylphenol	1.44	-1.84	-1.96	-1.98	-1.98	-2.04	
<u>37</u>	105-67-9	2,4-dimethylphenol	1.46	-1.96	-1.96	-1.96	-1.96	-2.03	
<u>38</u>	91-23-6	2-nitroanisole	1.09	-2.51	-2.66	-2.61	-2.34	-2.87	
<u>39</u>	95-51-2	2-chloroaniline	1.21	-2.26	-2.16	-2.17	-2.12	-2.27	
<u>40</u>	99-09-2	3-nitroaniline	0.93	-2.67	-2.85	-2.85	-2.42	-3.26	
<u>41</u>	539-03-7	4-chloroacetanilide	1.27	-2.37	-2.45	-2.32	-2.35	-2.29	
<u>42</u>	106-47-8	4-chloroaniline	1.16	-2.30	-2.21	-2.21	-2.17	-2.29	
<u>43</u>	62-53-3	aniline	0.35	-2.73	-2.69	-2.73	-2.77	-2.70	
<u>44</u>	60-80-0	antipyrine	0.22	-3.61	-3.48	-3.20	-3.55	-2.72	
<u>45</u>	119-61-9	benzophenone	2.06	-1.71	-1.88	-1.79	-1.92	-1.67	

Table 1. Cont.

No.	CAS No.		$\log k_{LAM}$	$\log K_p^{EPI}$	$\log K_p^{(9)}$	$\log K_p^{(11)}$	$\log K_p^{(12)}$	$\log K_p^{(13)}$	$\log K_p^{exp}$
46	120-51-4	benzyl benzoate	2.71	-1.36	-1.64	-1.50	-1.51	-1.51	
47	108-86-1	bromobenzene	1.75	-1.70	-1.57	-1.49	-1.59	-1.51	
48	68411-44-9	butylbenzene	2.78	-0.52	-0.84	-0.90	-0.96	-0.99	
49	495-40-9	butyrophenone	1.56	-1.80	-1.95	-1.99	-2.08	-1.92	
50	58-08-2	caffeine	-0.17	-3.94	-4.24	-3.71	-3.78	-3.47	
51	108-90-7	chlorobenzene	1.58	-1.55	-1.60	-1.57	-1.67	-1.59	
52	50-22-6	corticosterone	1.69	-3.46	-3.26	-3.25	-3.30	-2.92	
53	53-06-5	cortisone	1.29	-3.85	-3.75	-3.72	-3.67	-3.44	
54	50-28-2	estradiol	2.65	-1.67	-2.05	-1.96	-2.03	-1.80	-2.28
55	50-27-1	estriol	1.66	-2.80	-3.06	-2.93	-2.98	-2.68	
56	100-41-4	ethylbenzene	1.81	-1.31	-1.46	-1.48	-1.59	-1.48	
57	110-00-9	furan	0.32	-2.30	-2.38	-2.42	-2.46	-2.48	
58	106-24-1	geraniol	1.80	-1.36	-1.74	-1.91	-1.98	-1.86	
59	1671-75-6	heptanophenone	2.99	-1.13	-1.00	-1.16	-1.18	-1.20	
60	50-23-7	hydrocortisone	1.30	-3.77	-3.79	-3.76	-3.70	-3.50	-3.92
61	108-39-4	3-methylphenol	1.05	-2.11	-2.19	-2.19	-2.20	-2.24	
62	93-58-3	methyl benzoate	1.11	-2.16	-2.30	-2.29	-2.29	-2.32	
63	150-68-5	monuron	1.24	-2.63	-2.78	-2.51	-2.60	-2.37	
64	123-35-3	myrcene	3.01	-0.69	-0.56	-0.77	-0.82	-0.87	
65	95-53-4	o-toluidine	0.65	-2.53	-2.51	-2.49	-2.63	-2.37	
66	93-55-0	propiophenone	1.16	-2.10	-2.17	-2.21	-2.32	-2.12	
67	103-65-1	propylbenzene	2.29	-1.03	-1.16	-1.20	-1.28	-1.24	
68	106-42-3	p-xylene	1.83	-1.31	-1.46	-1.46	-1.57	-1.47	
69	289-95-2	pyrimidine	-0.50	-3.52	-3.28	-3.22	-3.31	-3.13	
70	120-80-9	pyrocatechol	0.49	-2.84	-2.75	-2.76	-2.63	-2.90	
71	109-97-7	pyrrole	0.18	-2.68	-2.64	-2.59	-2.65	-2.60	
72	91-22-5	quinoline	2.07	-2.18	-1.68	-1.51	-1.53	-1.59	
73	108-46-3	resorcinol	0.40	-2.89	-2.83	-2.82	-2.71	-2.95	-3.62
74	62-56-6	thiourea	-0.77	-3.95	-3.87	-3.96	-3.45	-4.43	
75	89-83-8	thymol	2.19	-1.45	-1.52	-1.57	-1.55	-1.66	-1.28
76	1009-14-9	valerophenone	2.01	-1.62	-1.63	-1.73	-1.80	-1.70	
77	109-66-0	pentane	2.28	-0.96	-0.89	-0.95	-0.87	-1.24	
78	75-09-2	dichloromethane	0.22	-2.45	-2.30	-2.34	-2.49	-2.28	
79	67-66-3	chloroform	0.62	-2.17	-2.12	-2.12	-2.26	-2.08	
80	56-23-5	carbon tetrachloride	1.61	-1.79	-1.48	-1.46	-1.50	-1.58	
81	1300-21-6	1,2-dichloroethane	0.34	-2.38	-2.28	-2.33	-2.51	-2.22	
82	79-34-5	1,1,2,2-tetrachloroethane	1.28	-2.16	-1.77	-1.78	-1.93	-1.75	
83	109-69-3	1-chlorobutane	1.05	-1.57	-1.76	-1.87	-1.99	-1.86	
84	60-29-7	diethyl ether	-0.06	-2.63	-2.69	-2.74	-2.91	-2.60	-2.80
85	111-43-3	dipropyl ether	0.78	-2.03	-2.16	-2.26	-2.41	-2.17	
86	79-20-9	methyl acetate	-0.66	-3.10	-3.23	-3.27	-3.33	-3.22	
87	141-78-6	ethyl acetate	-0.25	-2.82	-2.98	-3.04	-3.08	-3.01	
88	123-86-4	butyl acetate	0.62	-2.27	-2.24	-2.55	-2.55	-2.57	
89	75-05-8	acetonitrile	-0.70	-3.26	-3.13	-3.17	-3.19	-3.19	
90	107-12-0	propionitrile	-0.35	-3.01	-2.96	-2.98	-3.00	-3.01	
91	64-17-5	ethanol	-0.62	-3.27	-3.09	-3.10	-3.16	-3.08	-3.10
92	71-23-8	1-propanol	-0.42	-2.97	-2.99	-3.03	-3.11	-2.98	-2.92
93	75-65-0	2-methyl-2-propanol	0.37	-2.99	-2.51	-2.52	-2.52	-2.58	
94	71-41-0	1-pentanol	0.33	-2.30	-2.53	-2.62	-2.68	-2.60	-2.22
95	75-85-4	2-methyl-2-butanol	-0.08	-2.51	-2.88	-2.93	-3.05	-2.81	
96	111-27-3	1-hexanol	0.83	-2.03	-2.21	-2.33	-2.36	-2.35	-1.89
97	64-18-6	formic acid	-0.65	-3.42	-3.18	-3.21	-3.06	-3.42	
98	64-19-7	acetic acid	-0.68	-3.25	-3.29	-3.31	-3.21	-3.43	-3.21
99	79-09-4	propionic acid	-0.08	-3.00	-2.89	-2.94	-2.80	-3.13	
100	107-92-6	butanoic acid	0.38	-2.77	-2.59	-2.67	-2.51	-2.89	
101	109-99-9	tetrahydrofuran	-0.18	-2.90	-2.89	-2.79	-2.96	-2.66	
102	93-89-0	ethyl benzoate	1.48	-1.89	-2.08	-2.09	-2.08	-2.13	
103	88-73-3	1-chloro-2-nitrobenzene	1.44	-2.20	-2.20	-2.22	-1.98	-2.52	
104	140-29-4	phenylacetone	0.82	-2.43	-2.45	-2.44	-2.48	-2.42	
105	91-59-8	2-naphthylamine	1.77	-2.09	-2.08	-1.96	-1.97	-1.98	
106	108-43-0	3-chlorophenol	1.70	-1.87	-1.73	-1.71	-1.61	-1.91	
107	99-04-7	3-methylbenzoic acid	1.43	-2.00	-2.17	-2.15	-1.99	-2.36	
108	100-02-7	4-nitrophenol	1.28	-2.32	-2.52	-2.49	-2.04	-2.97	-2.25
109	17849-38-6	4-chlorobenzyl alcohol	1.06	-2.30	-2.29	-2.26	-2.32	-2.23	
110	541-73-1	1,3-dichlorobenzene	2.48	-1.28	-1.04	-0.98	-0.99	-1.14	
111	108-67-8	1,3,5-trimethylbenzene	2.61	-1.21	-0.98	-0.96	-1.00	-1.07	
112	142-82-5	heptane	3.20	-0.27	-0.30	-0.41	-0.29	-0.78	

Table 1. Cont.

No.	CAS No.		$\log k_{IAM}$	$\log K_p^{EPI}$	$\log K_p^{(9)}$	$\log K_p^{(11)}$	$\log K_p^{(12)}$	$\log K_p^{(13)}$	$\log K_p^{exp}$
113	110-54-3	hexane	1.97	-0.70	-1.17	-1.26	-1.28	-1.40	
114	103-90-2	acetaminophen	0.38	-3.35	-3.24	-3.13	-3.07	-3.12	
115	66085-59-4	nimodipine	3.06	-3.13	-2.88	-2.90	-2.45	-3.07	
116	57-83-0	progesterone	2.98	-2.00	-1.88	-1.85	-2.05	-1.52	
117	19387-91-8	tinidazole	0.26	-4.42	-4.15	-3.99	-3.63	-4.14	
118	106-49-0	p-toluidine	1.15	-2.48	-2.18	-2.21	-2.17	-2.30	
119	90-41-5	2-aminobiphenyl	2.13	-1.87	-1.82	-1.81	-1.83	-1.80	
120	103-69-5	N-ethylaniline	1.06	-2.05	-2.29	-2.23	-2.40	-2.08	
121	86-55-5	1-naphthoic acid	2.13	-1.71	-1.99	-1.85	-1.72	-2.01	
122	103-82-2	phenylacetic acid	0.76	-2.63	-2.68	-2.64	-2.58	-2.70	
123	1878-65-5	3-chlorophenylacetic acid	1.47	-2.37	-2.24	-2.20	-2.07	-2.34	
124	1821-12-1	4-phenylbutanoic acid	1.52	-2.12	-2.20	-2.23	-2.15	-2.32	
125	103-29-7	1,2-diphenylethane	3.77	-0.64	-0.53	-0.42	-0.49	-0.49	
126	58-22-0	testosterone	2.23	-2.22	-2.38	-2.31	-2.51	-1.96	
127	78-93-3	2-butanone	-0.38	-3.02	-2.91	-3.02	-3.16	-2.90	-2.95
128	110-86-1	pyridine	0.32	-2.82	-2.56	-2.52	-2.62	-2.47	
129	123-07-9	4-ethylphenol	1.54	-1.78	-1.88	-1.90	-1.89	-1.99	-1.46
130	645-56-7	4-propylphenol	2.02	-1.44	-1.57	-1.62	-1.58	-1.75	
131	1638-22-8	4-butylphenol	2.51	-1.22	-1.24	-1.33	-1.26	-1.50	
132	371-41-5	4-fluorophenol	0.96	-2.26	-2.14	-2.18	-2.15	-2.29	
133	106-41-2	4-bromophenol	1.81	-2.05	-1.74	-1.67	-1.59	-1.85	-1.44
134	540-38-5	4-iodophenol	2.10	-2.11	-1.65	-1.54	-1.47	-1.71	
135	103-79-7	benzyl methyl ketone	0.38	-2.60	-2.76	-2.78	-3.01	-2.52	
136	72509-76-3	felodipine	3.47	-2.40	-1.91	-1.86	-1.74	-1.84	
137	63675-72-9	nisoldipine	3.26	-2.82	-2.53	-2.56	-2.09	-2.80	
138	103890-78-4	lacidipine	4.00	-1.91	-2.04	-2.23	-2.11	-2.06	
139	738-70-5	trimethoprim	0.95	-3.83	-4.05	-3.88	-3.59	-3.87	
140	50-24-8	prednisolone	1.65	-3.75	-3.54	-3.50	-3.38	-3.32	
141	50-78-2	acetylsalicylic acid	0.82	-3.03	-3.01	-2.98	-2.73	-3.16	
142	65-85-0	benzoic acid	1.05	-2.25	-2.38	-2.36	-2.21	-2.56	
143	140-65-8	pramocaine	2.56	-2.17	-2.04	-2.02	-2.25	-1.67	
144	67-64-1	acetone	-0.75	-3.29	-3.13	-3.22	-3.37	-3.09	-3.21
145	123-30-8	4-aminophenol	-0.20	-3.39	-3.33	-3.36	-3.32	-3.35	
146	93-60-7	methyl nicotinate	0.27	-3.02	-3.04	-3.00	-2.99	-2.98	
147	68-12-2	N,N-dimethylformamide	-0.47	-3.89	-3.11	-3.11	-3.22	-3.01	
148	26839-75-8	timolol	0.90	-3.36	-3.82	-3.97	-3.69	-3.94	
149	2180-92-9	bupivacaine	1.88	-2.16	-2.56	-2.61	-2.98	-2.04	
150	721-50-6	prilocaine	0.99	-2.64	-3.01	-3.01	-3.20	-2.66	
151	29122-68-7	atenolol	0.65	-4.19	-3.71	-3.80	-3.70	-3.64	
152	525-66-6	propranolol	2.20	-1.95	-1.90	-2.30	-2.43	-2.05	
153	321-97-1	pseudoephedrine	0.36	-2.98	-3.07	-3.11	-3.30	-2.81	
154	37517-30-9	acebutolol	1.57	-3.56	-3.42	-3.48	-3.43	-3.23	
155	13655-52-2	alprenolol	2.08	-2.14	-2.16	-2.33	-2.43	-2.11	
156	37350-58-6	metoprolol	1.21	-3.06	-3.00	-3.10	-3.27	-2.72	
157	6452-71-7	oxprenolol	1.55	-2.90	-2.62	-2.84	-2.96	-2.55	
158	18559-94-9	albuterol	0.48	-3.73	-3.61	-3.70	-3.68	-3.50	
159	54910-89-3	fluoxetine	2.98	-2.00	-1.50	-1.54	-1.74	-1.28	
160	52-53-9	verapamil	2.76	-2.84	-2.94	-2.98	-3.38	-2.19	

Where:  $\log k_{IAM}$ —IAM HPLC retention factors [46];  $\log K_p^{exp}$ —experimental values [29];  $\log K_p^{EPI}$ —values calculated using DERMWIN software [12]; and  $\log K_p^{(9)}$  and  $\log K_p^{(11)}$  to  $\log K_p^{(13)}$ —values calculated according to Equations (9) and (11)–(13).

The compounds **1** to **160** were chromatographed on the IAM stationary phase using buffered aqueous mobile phases as described in Section 3. The retention factors ( $\log k_{IAM}$ ) were compiled from the published literature by Sprunger et al. [46] whose main objective was to propose an IAM chromatographic retention model based on Abraham's solvation parameters. In our investigations, we focused mainly on drugs (that are or potentially could be administered transdermally) and environmentally relevant compounds (organic pollutants whose skin absorption can be a possible route of exposure).  $\log k_{IAM}$  values taken from Reference [46] were correlated with the  $\log K_p^{EPI}$  values presented in Table 1. Unfortunately, the resulting linear correlation (7) is poor, with  $R^2 = 0.46$ .

$$\log K_p^{EPI} = -2.98 (\pm 0.07) + 0.52 (\pm 0.04) \log k_{IAM} \quad (7)$$

$(n = 160, R^2 = 0.46, R^2_{adj.} = 0.45, MSE = 0.32, F = 132.7, p < 0.01, s_e = 0.57)$

Previous studies of the relationships between  $\log K_p$  and  $\log k_{IAM}$  (e.g., Equation (8)) for small groups of compounds [31,34,36] failed to provide general chromatographic models applicable to molecules from different chemical classes:

$$\log K_p = -5.154 + 1.443 \log k_{IAM} \quad (8)$$

$(n = 32, R^2 = 0.26)$

From this (and Equation (5) [31]), it was concluded that  $\log k_{IAM}$  obtained as described in Section 3 is not sufficient as a sole predictor of  $\log K_p$ . At this point, it was decided to seek a multivariate linear relationship that would meet the following requirements: (i) give the best possible fit with the  $\log K_p^{EPI}$  reference values; (ii) fit the experimental  $\log K_p^{exp}$  values for a subgroup of compounds whose experimental skin permeability data are available (preferably from a single source to avoid possible discrepancies between experimental data collected by different protocols); and (iii) be as simple as possible and contain the minimum number of independent variables needed to generate models of reasonable predictive power without the risk of overfitting. These goals were achieved in our study by taking the following steps:

- a. Generating a well-fitting model based on a relatively large number of independent variables selected by forward stepwise multiple regression;
- b. Validation of the model using two randomly selected subsets of compounds, namely a training set ( $n = 120$ ) and a test set ( $n = 40$ );
- c. Validation of the initial model using experimental  $\log K_p^{exp}$  data for a subset of compounds ( $n = 20$ );
- d. Analysis of every step of multiple stepwise regression in order to eliminate redundant independent variables; and
- e. Building a new model based on a reduced set of independent variables and its validation as described above.

In the first step of the multiple regression analysis, the calculated physicochemical parameters presented in Table 2 were incorporated by forward stepwise multiple regression (Equation (9), Figure 1):

$$\log K_p^{EPI} = -1.66 (\pm 0.30) + 0.75 (\pm 0.03) \log k_{IAM} - 0.0034 (\pm 0.002) PSA + 0.033 (\pm 0.016) FRB - 0.089 (\pm 0.035) HA + 0.0090 (\pm 0.003) V_M - 0.092 (\pm 0.021) \alpha + 0.035 (\pm 0.028) E_{HOMO} - 0.031 (\pm 0.024) E_{LUMO} - 0.0022 (\pm 0.0008) S_a \quad (9)$$

$(n = 160, R^2 = 0.96, R^2_{adj} = 0.92, MSE = 0.043, F = 216.6, p < 0.01, s_e = 0.21)$

**Table 2.** Calculated descriptors for compounds 1 to 160.

		PSA	FRB	HA	$V_M$	$\alpha$	$E_{HOMO}$	$E_{LUMO}$	$S_a$
<u>1</u>	Acetanilide	29.1	1	2	122.5	16.07	-8.82	-0.03	312.2
<u>2</u>	Acetophenone	17.1	1	1	121.0	14.38	-10.00	-0.44	293.2
<u>3</u>	2-aminophenol	46.3	2	2	90.1	12.83	-8.10	0.52	264.6
<u>4</u>	Anisole	9.2	1	1	113.4	13.05	-9.11	0.35	283.9
<u>5</u>	Benzaldehyde	17.1	1	1	101.1	13.08	-10.05	-0.48	266.7
<u>6</u>	Benzamide	43.1	1	2	108.1	13.95	-9.72	-0.36	286.2
<u>7</u>	Benzene	0.0	0	0	89.4	10.41	-9.75	0.40	241.1
<u>8</u>	Benzonitrile	23.8	0	1	100.0	12.42	-10.10	-0.58	271.7
<u>9</u>	Benzyl alcohol	20.2	2	1	109.3	12.09	-9.58	0.33	281.5
<u>10</u>	Biphenyl	0.0	0	0	154.7	20.16	-8.92	-0.36	345.0
<u>11</u>	1-bromonaphthalene	0.0	0	0	139.7	20.53	-8.99	-0.65	328.6
<u>12</u>	3-bromophenol	20.2	1	1	104.1	14.20	-9.41	-0.13	282.5
<u>13</u>	Cinnamyl alcohol	20.2	3	1	127.9	17.32	-8.95	-0.15	329.7
<u>14</u>	Coumarin	26.3	0	2	117.1	15.76	-9.45	-0.99	305.5
<u>15</u>	Cyclohexanone	17.1	0	1	103.0	11.02	-10.48	0.85	256.1
<u>16</u>	Diethyl phtalate	52.6	6	4	198.2	23.42	-10.24	-0.93	407.7
<u>17</u>	2,6-dimethylphenol	20.2	1	1	120.4	14.98	-8.96	0.29	296.7
<u>18</u>	4-hydroxybenzyl alcohol	40.5	3	2	101.7	13.71	-9.06	0.31	291.5

Table 2. Cont.

		PSA	FRB	HA	$V_M$	$\alpha$	$E_{HOMO}$	$E_{LUMO}$	$S_a$
<u>19</u>	2-methylphenol	20.2	1	1	104.1	13.07	−9.06	0.28	275.6
<u>20</u>	4-methylphenol	20.2	1	1	104.1	13.07	−8.95	0.33	274.0
<u>21</u>	Naphtalene	0.0	0	0	123.6	17.48	−8.84	−0.41	299.8
<u>22</u>	1-naphthol	20.2	1	1	122.0	18.23	−8.54	−0.36	308.8
<u>23</u>	2-naphthol	20.2	1	1	122.0	18.23	−8.72	−0.45	311.6
<u>24</u>	2-nitroaniline	71.8	2	4	103.6	14.68	−8.75	−0.82	306.6
<u>25</u>	4-nitroaniline	71.8	2	4	103.6	14.68	−9.00	−0.78	291.6
<u>26</u>	Nitrobenzene	45.8	1	3	101.3	13.00	−10.60	−1.14	273.3
<u>27</u>	4-nitrobenzyl alcohol	66.1	3	4	115.1	15.56	−10.52	−1.13	315.5
<u>28</u>	1-nitrobutane	45.8	3	3	107.3	10.55	−12.01	0.06	275.0
<u>29</u>	4-nitrotoluene	45.8	1	3	117.6	14.91	−10.47	−1.11	299.3
<u>30</u>	Phenol	20.2	1	1	87.9	11.15	−9.18	0.29	248.4
<u>31</u>	2-phenylethanol	20.2	3	1	119.8	14.80	−9.55	0.29	312.0
<u>32</u>	4-phenylphenol	20.2	2	1	153.2	20.90	−8.64	−0.34	355.8
<u>33</u>	Toluene	0.0	0	0	105.7	12.32	−9.44	0.45	265.6
<u>34</u>	4-chlorophenol	20.2	1	1	99.8	13.09	−9.01	0.05	272.4
<u>35</u>	2,3-benzofuran	13.1	0	1	106.3	14.43	−9.07	−0.15	216.7
<u>36</u>	2,3-dimethylphenol	20.2	1	1	120.4	14.98	−9.00	0.29	293.8
<u>37</u>	2,4-dimethylphenol	20.2	1	1	120.4	14.98	−8.86	0.31	301.2
<u>38</u>	2-nitroanisole	55.1	2	4	125.3	15.65	−10.29	−0.89	316.0
<u>39</u>	2-chloroaniline	26.0	1	1	103.7	14.03	−8.17	0.31	277.6
<u>40</u>	3-nitroaniline	71.8	2	4	103.6	14.68	−9.28	−1.06	291.8
<u>41</u>	4-chloroacetanilide	29.1	1	2	134.5	18.01	−8.67	−0.06	341.5
<u>42</u>	4-chloroaniline	26.0	1	1	103.7	14.03	−8.11	0.38	282.0
<u>43</u>	Aniline	26.0	1	1	91.7	12.09	−8.07	0.62	257.9
<u>44</u>	Antipyrine	23.6	1	3	162.8	21.63	−9.04	−0.33	383.0
<u>45</u>	Benzophenone	17.1	2	1	167.6	22.22	−9.94	−0.67	374.7
<u>46</u>	Benzyl benzoate	26.3	4	2	188.0	24.78	−9.61	−0.34	438.6
<u>47</u>	Bromobenzene	0.0	0	0	105.6	13.46	−9.81	−0.05	273.0
<u>48</u>	Butylbenzene	0.0	3	0	155.3	17.87	−9.51	0.36	357.3
<u>49</u>	Butyrophenone	17.1	3	1	154.0	18.06	−9.99	−0.09	363.0
<u>50</u>	Caffeine	53.5	0	6	133.4	19.97	−8.89	−0.49	364.0
<u>51</u>	Chlorobenzene	0.0	0	0	101.4	12.36	−9.39	0.06	264.1
<u>52</u>	Corticosterone	74.6	4	4	284.3	37.27	−10.21	−0.15	531.3
<u>53</u>	Cortisone	91.7	4	5	280.3	37.33	−10.09	−0.07	533.8
<u>54</u>	Estradiol	40.5	2	2	232.6	31.52	−8.86	−0.35	468.3
<u>55</u>	Estriol	60.7	3	3	229.6	32.15	−8.88	0.34	481.2
<u>56</u>	Ethylbenzene	0.0	1	0	122.3	14.19	−9.51	0.38	294.0
<u>57</u>	Furan	13.1	0	1	72.2	7.35	−9.38	0.61	208.2
<u>58</u>	Geraniol	20.2	5	1	177.9	19.71	−9.33	0.99	397.4
<u>59</u>	Heptanophenone	17.1	6	1	203.5	23.57	−10.00	−0.42	438.5
<u>60</u>	Hydrocortisone	94.8	5	5	281.4	37.89	−10.25	−0.18	542.9
<u>61</u>	3-methylphenol	20.2	1	1	104.1	13.07	−9.09	0.29	275.6
<u>62</u>	Methyl benzoate	26.3	2	2	127.3	15.07	−10.11	−0.46	314.4
<u>63</u>	Monuron	32.2	1	3	158.2	21.32	−9.13	−0.20	387.9
<u>64</u>	Myrcene	0.0	4	0	177.0	18.86	−9.28	0.29	374.8
<u>65</u>	o-toluidine	16.0	1	1	108.0	14.00	−7.99	0.59	276.9
<u>66</u>	Propiophenone	17.1	2	1	137.5	16.22	−9.99	−0.42	322.0
<u>67</u>	Propylbenzene	0.0	2	0	138.8	16.03	−9.51	0.37	326.6
<u>68</u>	p-xylene	0.0	0	0	122.0	14.23	−9.18	0.36	289.8
<u>69</u>	Pyrimidine	25.8	0	2	75.9	8.89	−10.29	−0.41	226.2
<u>70</u>	Pyrocatechol	40.5	2	2	86.3	11.90	−9.07	0.26	257.3
<u>71</u>	Pyrrole	15.8	0	1	67.8	8.20	−8.93	1.11	216.7
<u>72</u>	Quinoline	12.9	0	1	116.8	16.72	−9.24	−0.65	297.7
<u>73</u>	Resorcinol	40.5	2	2	86.3	11.90	−9.06	0.27	259.6
<u>74</u>	Thiourea	88.7	0	2	29.9	7.26	−8.62	−0.27	212.2
<u>75</u>	Thymol	20.2	2	1	154.2	18.69	−9.00	0.28	346.2
<u>76</u>	Valerophenone	17.1	4	1	170.5	19.89	−9.99	−0.42	379.6

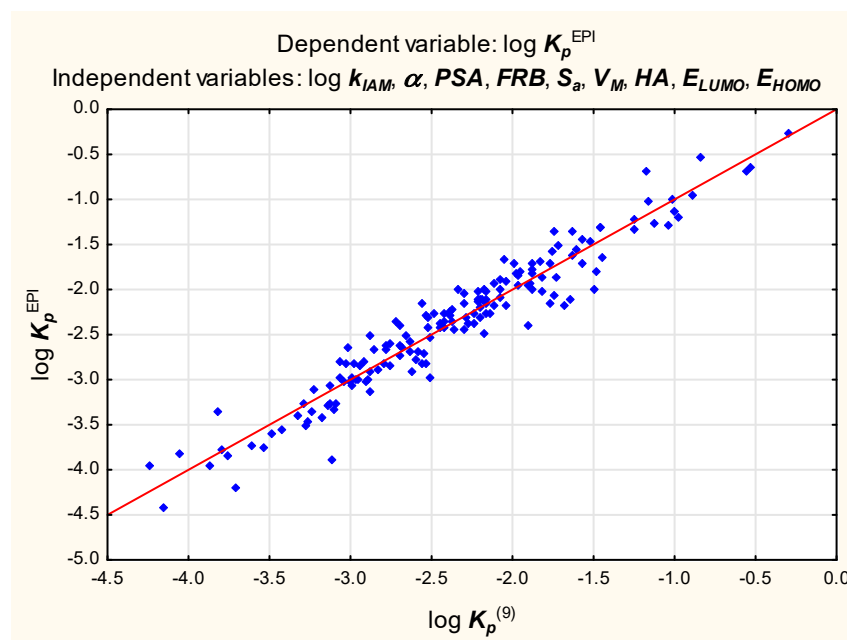
Table 2. Cont.

		PSA	FRB	HA	$V_M$	$\alpha$	$E_{HOMO}$	$E_{LUMO}$	$S_a$
77	Pentane	0.0	2	0	111.1	10.00	−11.30	3.45	266.9
78	Dichloromethane	0.0	0	0	67.8	6.49	−10.48	0.52	199.3
79	Chloroform	0.0	0	0	79.6	8.40	−10.88	−0.12	224.5
80	Carbon tetrachloride	0.0	0	0	90.6	10.32	−10.99	−0.63	244.2
81	1,2-dichloroethane	0.0	1	0	84.3	8.33	−10.69	0.54	231.1
82	1,1,2,2,-tetrachloroethane	0.0	1	0	107.8	12.14	−10.74	0.02	267.0
83	1-chlorobutane	0.0	2	0	106.0	10.08	−10.31	1.23	264.9
84	Diethyl ether	9.2	2	1	100.9	8.85	−10.48	2.86	260.9
85	Dipropyl ether	9.2	4	1	133.9	12.52	−10.49	2.76	317.2
86	Methyl acetate	26.3	1	2	81.5	7.03	−11.26	1.02	228.3
87	Ethyl acetate	26.3	2	2	98.0	8.83	−11.24	1.06	263.0
88	Butyl acetate	26.3	4	2	131.0	12.54	−11.25	1.05	232.4
89	Acetonitrile	23.8	0	1	54.9	4.45	−12.33	1.40	176.4
90	Propionitrile	23.8	0	1	71.4	6.29	−12.01	1.42	211.9
91	Ethanol	20.2	1	1	59.1	5.09	−10.90	3.33	191.0
92	1-propanol	20.2	2	1	75.6	6.93	−10.88	3.23	220.6
93	2-methyl-2-propanol	20.2	1	1	92.1	8.75	−11.28	3.26	244.4
94	1-pentanol	20.2	4	1	108.6	10.60	−10.89	3.11	281.4
95	2-methyl-2-butanol	20.2	2	1	108.6	10.59	−11.13	3.17	264.1
96	1-hexanol	20.2	5	1	125.1	12.44	−10.89	3.09	313.0
97	Formic acid	37.3	0	2	39.9	3.33	−11.57	0.97	158.3
98	Acetic acid	37.3	0	2	56.2	5.11	−11.43	0.93	192.8
99	Propionic acid	37.3	1	2	72.7	6.94	−11.31	0.96	222.4
100	Butanoic acid	37.3	2	2	89.2	8.78	−11.34	0.97	249.1
101	Tetrahydrofuran	9.2	0	1	79.8	7.95	−10.28	3.29	225.0
102	Ethyl benzoate	26.3	3	2	143.8	16.91	−10.08	−0.43	348.2
103	2-chloro-1-nitrobenzene	45.8	3	3	113.2	14.94	−9.94	−1.27	290.8
104	Phenylacetonitrile	23.8	1	1	115.7	14.16	−9.99	−0.09	300.7
105	2-naphthylamine	26.0	1	1	125.8	19.16	−7.92	−0.21	319.6
106	3-chlorophenol	20.2	1	1	99.8	13.09	−9.24	−0.01	272.6
107	3-methylbenzoic acid	37.3	1	2	118.2	15.07	−9.82	−0.49	304.5
108	4-nitrophenol	66.1	2	4	99.7	13.75	−10.17	−1.08	283.4
109	4-chlorobenzyl alcohol	20.2	2	1	115.2	14.91	−9.28	0.02	306.2
110	1,3-dichlorobenzene	0.0	0	0	113.3	14.29	−9.42	−0.19	288.6
111	1,3,5-trimethylbenzene	0.0	0	0	138.3	16.15	−9.28	0.44	320.3
112	Heptane	0.0	4	0	144.1	13.67	−11.27	3.30	327.7
113	Hexane	0.0	3	0	127.6	11.83	−11.28	3.36	297.7
114	Acetaminophen	49.3	1	3	121.0	16.81	−8.56	−0.02	323.6
115	Nimodipine	119.7	10	9	345.0	42.87	−9.21	−0.66	682.0
116	Progesterone	34.1	1	2	289.0	36.06	−10.14	−0.10	514.8
117	Tinidazole	101.2	5	7	172.4	23.36	−10.47	−1.21	432.8
118	p-toluidine	26.0	1	1	108.0	14.00	−7.95	0.64	285.0
119	2-aminobiphenyl	26.0	2	1	157.0	21.84	−7.98	−0.21	356.8
120	N-ethylaniline	12.0	2	1	125.4	16.05	−8.50	0.45	322.8
121	1-naphthoic acid	37.3	1	2	136.1	20.23	−9.13	−0.97	334.0
122	Phenylacetic acid	37.3	2	2	116.9	14.81	−9.81	0.22	313.7
123	3-chlorophenylacetic acid	37.3	2	2	128.8	16.75	−9.52	−0.20	337.0
124	4-phenylbutanoic acid	37.3	4	2	149.9	18.49	−9.67	0.21	372.0
125	1,2-diphenylethane	0.0	2	0	183.0	23.90	−9.48	0.32	402.0
126	Testosterone	37.3	1	2	257.0	32.95	−10.12	−0.09	477.5
127	2-butanone	17.1	1	1	91.7	8.17	−10.65	0.83	239.1
128	Pyridine	12.9	0	1	82.7	9.65	−10.10	0.01	231.9
129	4-ethylphenol	20.2	2	1	120.7	14.94	−9.00	0.32	305.7
130	4-propylphenol	20.2	3	1	137.2	16.78	−9.00	0.32	335.7
131	4-butylphenol	20.2	4	1	153.7	18.61	−8.99	0.32	360.8
132	4-fluorophenol	20.2	1	1	92.1	11.15	−9.27	−0.06	254.4



Table 2. Cont.

		PSA	FRB	HA	$V_M$	$\alpha$	$E_{HOMO}$	$E_{LUMO}$	$S_a$
<u>133</u>	4-bromophenol	20.2	1	1	104.1	14.20	−9.31	−0.03	283.6
<u>134</u>	4-iodophenol	20.2	1	1	109.9	16.27	−8.84	−0.41	289.8
<u>135</u>	Benzyl methyl ketone	17.1	2	1	135.9	16.04	−9.71	0.07	320.4
<u>136</u>	Felodipine	64.6	6	5	300.8	37.97	−8.87	−0.18	588.5
<u>137</u>	Nisoldipine	110.5	8	8	322.2	40.34	−9.15	−0.73	628.4
<u>138</u>	Lacidipine	90.9	11	7	404.0	50.26	−8.91	−1.29	706.6
<u>139</u>	Trimethoprin	105.5	5	7	231.9	31.82	−8.73	−0.07	519.0
<u>140</u>	Prednisolone	94.8	5	5	274.7	37.85	−10.07	−0.42	527.4
<u>141</u>	Acetylsalicylic acid	63.6	3	4	139.6	17.65	−10.19	−0.54	355.9
<u>142</u>	Benzoic acid	37.3	1	2	102.0	13.15	−10.13	−0.53	278.6
<u>143</u>	Pramocaine	30.9	9	4	284.6	33.45	−8.78	0.24	595.7
<u>144</u>	Acetone	17.1	0	1	75.2	6.33	−10.76	0.80	206.7
<u>145</u>	4-aminophenol	46.3	2	2	90.1	12.83	−7.84	0.46	267.6
<u>146</u>	Methyl nicotinate	39.2	2	3	120.6	14.32	−10.44	−0.80	310.4
<u>147</u>	N,N-dimethylformamide	20.3	0	2	82.6	7.87	−9.26	1.36	228.9
<u>148</u>	Timolol	108.0	8	7	258.5	32.57	−9.24	−1.05	520.8
<u>149</u>	Bupivacaine	32.3	5	3	279.2	35.13	−7.46	−0.40	514.1
<u>150</u>	Prilocaine	41.1	5	3	214.0	26.73	−9.23	0.18	449.6
<u>151</u>	Atenolol	84.6	9	5	236.7	29.44	−9.30	−0.03	541.0
<u>152</u>	Propranolol	41.5	7	3	237.2	31.31	−8.62	−0.43	307.7
<u>153</u>	Pseudoefedrine	32.3	4	2	162.7	19.88	−9.44	0.29	371.4
<u>154</u>	Acebutolol	87.7	11	6	300.7	37.55	−9.15	−0.43	642.5
<u>155</u>	Alprenolol	41.5	9	3	247.5	29.75	−9.12	0.26	506.5
<u>156</u>	Metoprolol	50.7	10	4	258.7	30.55	−9.00	−0.27	569.8
<u>157</u>	Oxprenolol	50.7	10	4	255.2	30.45	−9.21	0.12	496.3
<u>158</u>	Albuterol	72.7	8	4	207.6	26.86	−8.97	0.16	474.7
<u>159</u>	Fluoxetine	21.3	6	2	266.7	31.67	−9.44	−0.39	541.6
<u>160</u>	Verapamil	64.0	13	6	429.4	52.28	−8.78	−0.95	817.4

Figure 1. Equation (9)—reference vs. predicted  $\log K_p$  values.

The model (9) was validated using the holdout method in which data points are assigned to two sets usually called the training set and the test set. The size of each set is arbitrary (the test set is usually smaller than the training set). The group of 160 studied compounds was divided into two subsets: a training set (1 to 120) and a test set (121 to

**160).** The Equation (10) generated for the training set and containing the same independent variables as Equation (9) is as follows:

$$\log K_p^{\text{EPI}} = -1.71 (\pm 0.35) + 0.76 (\pm 0.03) \log k_{IAM} - 0.0042 (\pm 0.002) PSA + 0.038 (\pm 0.02) FRB - 0.074 (\pm 0.035) HA + 0.0087 (\pm 0.003) V_M - 0.11 (\pm 0.02) \alpha + 0.050 (\pm 0.029) E_{HOMO} - 0.028 (\pm 0.023) E_{LUMO} - 0.00053 (\pm 0.00138) S_a \quad (10)$$

( $n = 120, R^2 = 0.95, R^2_{\text{adj.}} = 0.94, \text{MSE} = 0.032, F = 210.5, p < 0.01, s_e = 0.18$ )

The values of  $\log K_p^{(10)}$  were calculated for the test set according to Equation (10) and plotted against the reference  $\log K_p^{\text{EPI}}$  values to furnish a linear relationship ( $R^2 = 0.87$ ). The model (9) was also tested on the subgroup of 20 compounds whose  $\log K_p^{\text{exp}}$  values were available (16 compounds belonging to the training set and four compounds belonging to the test set). The resulting relationship between  $\log K_p^{(9)}$  and  $\log K_p^{\text{exp}}$  is linear, with  $R^2 = 0.90$ .

Equation (9), despite encouraging results of validation, was found unsatisfying because it seems over-parameterized; it contains nine independent variables whose contributions, apart from  $\log k_{IAM}$ ,  $\alpha$  and  $PSA$ , are negligible ( $\log k_{IAM}$ ,  $\alpha$  and  $PSA$  account for over 91% of the total variability and the remaining six variables for less than 4%). With so many independent variables, it is also difficult to avoid colinearity. A decision was made to simplify Equation (9) as much as possible; apart from  $\log k_{IAM}$ , only two variables— $PSA$  and  $\alpha$ —seem to have a sufficient influence on  $\log K_p$  to justify incorporating them in Equations (11)–(13) (Figures 2–4).

$$\log K_p^{\text{EPI}} = -2.22 (\pm 0.04) + 0.75 (\pm 0.03) \log k_{IAM} - 0.042 (\pm 0.004) \alpha - 0.0096 (\pm 0.0011) PSA \quad (11)$$

( $n = 160, R^2 = 0.91, R^2_{\text{adj.}} = 0.91, \text{MSE} = 0.052, F = 538.9, p < 0.01, s_e = 0.23$ )

$$\log K_p^{\text{EPI}} = -2.24 (\pm 0.05) + 0.91 (\pm 0.03) \log k_{IAM} - 0.070 (\pm 0.003) \alpha \quad (12)$$

( $n = 160, R^2 = 0.87, R^2_{\text{adj.}} = 0.87, \text{MSE} = 0.078, F = 524.7, p < 0.01, s_e = 0.28$ )

$$\log K_p^{\text{EPI}} = -2.39 (\pm 0.05) + 0.51 (\pm 0.02) \log k_{IAM} - 0.019 (\pm 0.001) PSA \quad (13)$$

( $n = 160, R^2 = 0.85, R^2_{\text{adj.}} = 0.85, \text{MSE} = 0.088, F = 452.8, p < 0.01, s_e = 0.30$ )

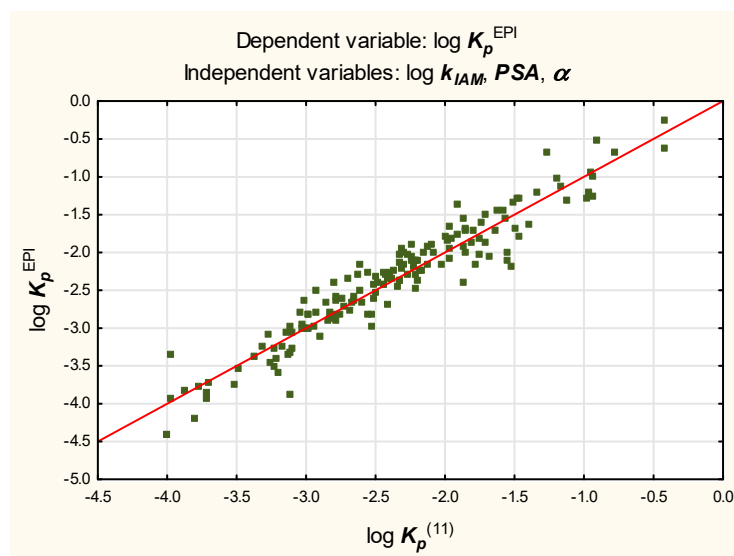


**Figure 2.** Equation (11)—reference vs. predicted  $\log K_p$  values.

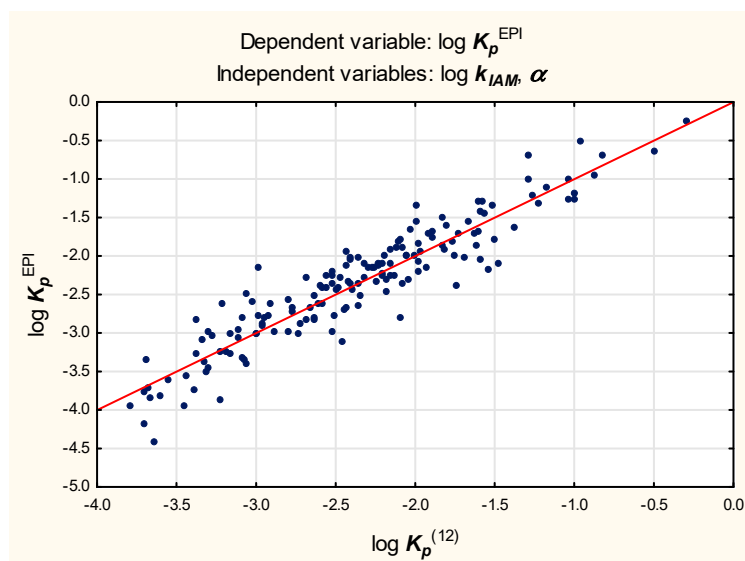


Figure 3. Equation (12)—reference vs. predicted  $\log K_p$  values.

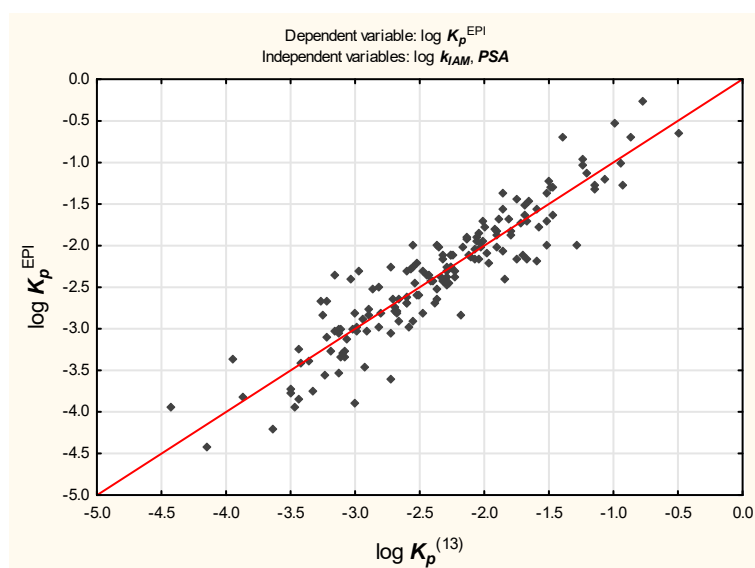


Figure 4. Equation (13)—reference vs. predicted  $\log K_p$  values.

The group of 160 studied compounds was divided into two subsets: a training set (**1** to **120**) and a test set (**121** to **160**). The Equations (14)–(16), generated for the training set and containing the same independent variables as Equations (11)–(13), are as follows:

$$\log K_p^{\text{EPI}} = -2.17 (\pm 0.05) + 0.79 (\pm 0.03) \log k_{IAM} - 0.0086 (\pm 0.0012) PSA - 0.051 (\pm 0.005) \alpha \quad (14)$$

( $n = 120$ ,  $R^2 = 0.93$ ,  $R^2_{\text{adj.}} = 0.93$ ,  $\text{MSE} = 0.042$ ,  $F = 490.7$ ,  $p < 0.01$ ,  $s_e = 0.21$ )

$$\log K_p^{\text{EPI}} = -2.17 (\pm 0.05) + 0.95 (\pm 0.03) \log k_{IAM} - 0.077 (\pm 0.004) \alpha \quad (15)$$

( $n = 120$ ,  $R^2 = 0.90$ ,  $R^2_{\text{adj.}} = 0.89$ ,  $\text{MSE} = 0.060$ ,  $F = 500.1$ ,  $p < 0.01$ ,  $s_e = 0.25$ )

$$\log K_p^{\text{EPI}} = -2.41 (\pm 0.05) + 0.53 (\pm 0.03) \log k_{IAM} - 0.017 (\pm 0.001) PSA \quad (16)$$

( $n = 120$ ,  $R^2 = 0.87$ ,  $R^2_{\text{adj.}} = 0.86$ ,  $\text{MSE} = 0.077$ ,  $F = 375.2$ ,  $p < 0.01$ ,  $s_e = 0.28$ )

The values of  $\log K_p^{(14)}$ ,  $\log K_p^{(15)}$ , and  $\log K_p^{(16)}$  were calculated for the test set according to Equations (14)–(16) and plotted against the reference  $\log K_p^{\text{EPI}}$  values to furnish linear relationships ( $R^2 = 0.86$ ,  $0.79$ , and  $0.83$ , respectively). The models (11), (12), and (13) were also tested on the subgroup of 20 compounds whose  $\log K_p^{\text{exp}}$  values were

available. The resulting relationships between  $\log K_p^{(11)}$ ,  $\log K_p^{(12)}$ , and  $\log K_p^{(13)}$ —as well as  $\log K_p^{\text{exp}}$ —are linear, with  $R^2 = 0.88$ ,  $0.84$ , and  $0.80$ , respectively.

Equation (13) involves  $\log k_{IAM}$ , which encodes some important properties responsible for drugs' absorption (lipophilicity and molecular size), but accounts for only 46% of the total  $\log K_p$  variability and  $PSA$ , which is known to influence other absorption phenomena (e.g., transport through the blood–brain barrier and uptake from a gastrointestinal tract) [47–49]. A coefficient for  $PSA$  in Equation (13) is negative, which suggests (as already reported, e.g., for the blood–brain barrier passage or oral absorption) that compounds with large polar surface areas are not easily absorbed through skin. However, from the statistical point of view, Equation (11) is superior to Equations (12) and (13), and gives results comparable to those obtained using Equation (9) without the risk of overfitting.

### 3. Materials and Methods

#### 3.1. IAM Chromatography

The chromatographic retention factors ( $\log k_{IAM}$ ) for the compounds analyzed in this study were compiled by Sprunger et al. [46]. They were obtained on a IAM.PC.DD2 HPLC column using an aqueous mobile phase buffered at  $\text{pH} \leq 3$  for carboxylic acids and in the  $\text{pH}$  range of 6.5 to 7.5 for other compounds.

#### 3.2. Calculated Molecular Descriptors

The molecular descriptors for the compounds investigated during this study were calculated with HyperChem 8.0 utilizing the PM3 semi-empirical method with Polak–Ribiere's algorithm: total dipole moment— $DM$  (D), surface area (grid)— $S_a$  ( $\text{\AA}^2$ ), molecular weight— $M_w$  ( $\text{g mol}^{-1}$ ), energy of the highest occupied molecular orbital— $E_{HOMO}$  (eV), and energy of the lowest unoccupied molecular orbital— $E_{LUMO}$  (eV). Other physicochemical parameters (octanol-water partition coefficient— $\log P$ , polar surface area— $PSA$  ( $\text{\AA}^2$ ), H-bond donor count— $HD$ , H-bond acceptor count— $HA$ , polarizability— $\alpha$  ( $\text{cm}^3$ ), molar volume— $V_M$  ( $\text{cm}^3$ ), and freely rotatable bond count— $FRB$ ) were calculated using ACD/Labs 8.0 software. ( $N+O$ ), which is the total nitrogen and oxygen atom count, was calculated from the molecular structures. The relevant calculated molecular descriptors are given in Table 2. Statistical analysis was done using Statistica v.13 or StatistiXL v.2.

### 4. Conclusions

Multiple regression models for predicting the skin permeability coefficient of structurally diverse compounds were developed.

Due to the limited availability of experimental permeability data for the solutes investigated in this study, the reference skin permeability coefficients were calculated according to a widely accepted theoretical model proposed by Potts. The values of  $\log K_p$  obtained using this model are in good agreement with the experimental data for drug-like compounds.

The newly developed  $\log K_p$  models are based on a set of IAM chromatographic and computational descriptors. The main descriptors, responsible for the variability of  $\log K_p$  in MLR equations, are  $\log k_{IAM}$ , polarizability ( $\alpha$ ), and polar surface area ( $PSA$ ), and the MLR model gains very little in predictive power when other descriptors are incorporated. Linear relationships based on the IAM chromatographic retention factor and readily available calculated physico-chemical parameters give very good results and have the benefit of simplicity. The proposed models may be applied during the early steps of the drug discovery process when different drugs' physico-chemical and biological properties are often studied in vitro using IAM chromatography and rapid predictions are required. IAM chromatographic and computational studies of the skin permeability of compounds may therefore be of interest to pharmaceutical and medicinal chemists, and to researchers in the area of environmental sciences since many compounds of environmental concern are absorbed through skin.

**Author Contributions:** Conceptualization, A.W.S.; methodology, A.W.S. and E.B.; investigation, A.W.S.; writing—original draft preparation, A.W.S. All authors have read and agreed to the published version of the manuscript.

**Funding:** This research study was supported by an internal grant of the Medical University of Łódź, no. 503/3-016-03/503-31-001.

**Institutional Review Board Statement:** Not applicable.

**Informed Consent Statement:** Not applicable.

**Data Availability Statement:** Data generated in this study can be found in this manuscript.

**Conflicts of Interest:** The authors declare no conflict of interest. The funders had no role in the design of the study; in the collection, analyses, or interpretation of data; in the writing of the manuscript, or in the decision to publish the results.

**Sample Availability:** Not applicable.

## References

1. Todo, H. Transdermal Permeation of Drugs in Various Animal Species. *Pharmaceutics* **2017**, *9*, 33. [CrossRef]
2. Neupane, R.; Boddu, S.H.S.; Renukuntla, J.; Babu, R.J.; Tiwari, A.K. Alternatives to Biological Skin in Permeation Studies: Current Trends and Possibilities. *Pharmaceutics* **2020**, *12*, 152. [CrossRef]
3. Potts, R.O.; Guy, R.H. Predicting Skin Permeability. *Pharm. Res.* **1992**, *9*, 663–669. [CrossRef] [PubMed]
4. Lian, G.; Chen, L.; Han, L. An Evaluation of Mathematical Models for Predicting Skin Permeability. *J. Pharm. Sci.* **2008**, *97*, 584–598. [CrossRef] [PubMed]
5. Cronin, M.T.D.; Dearden, J.C.; Moss, G.P.; Murray-Dickson, G. Investigation of the Mechanism of Flux across Human Skin in Vitro by Quantitative Structure–Permeability Relationships. *Eur. J. Pharm. Sci.* **1999**, *7*, 325–330. [CrossRef]
6. Fu, X.C.; Wang, G.P.; Wang, Y.F.; Liang, W.Q.; Yu, Q.S.; Chow, M.S.S. Limitation of Potts and Guy’s Model and a Predictive Algorithm for Skin Permeability Including the Effects of Hydrogen-Bond on Diffusivity. *Die Pharm. Int. J. Pharm. Sci.* **2004**, *59*, 282–285.
7. Mitragotri, S.; Anissimov, Y.G.; Bunge, A.L.; Frasch, H.F.; Guy, R.H.; Hadgraft, J.; Kasting, G.B.; Lane, M.E.; Roberts, M.S. Mathematical Models of Skin Permeability: An Overview. *Int. J. Pharm.* **2011**, *418*, 115–129. [CrossRef] [PubMed]
8. Naseem, S.; Zushi, Y.; Nabi, D. Development and Evaluation of Two-Parameter Linear Free Energy Models for the Prediction of Human Skin Permeability Coefficient of Neutral Organic Chemicals. *J. Cheminform.* **2021**, *13*, 25. [CrossRef] [PubMed]
9. Lipinski, C.A. Rule of Five in 2015 and beyond: Target and Ligand Structural Limitations, Ligand Chemistry Structure and Drug Discovery Project Decisions. *Adv. Drug Deliv. Rev.* **2016**, *101*, 34–41. [CrossRef] [PubMed]
10. Lipinski, C.A. Lead- and Drug-like Compounds: The Rule-of-Five Revolution. *Drug Discov. Today Technol.* **2004**, *1*, 337–341. [CrossRef] [PubMed]
11. Daina, A.; Michielin, O.; Zoete, V. SwissADME: A Free Web Tool to Evaluate Pharmacokinetics, Drug-Likeness and Medicinal Chemistry Friendliness of Small Molecules. *Sci. Rep.* **2017**, *7*, 42717. [CrossRef] [PubMed]
12. US EPA. EPI Suite™-Estimation Program Interface. Available online: <https://www.epa.gov/tsc-screening-tools/epi-suite-estimation-program-interface> (accessed on 11 March 2022).
13. Abraham, M.; Martins, F.; Mitchell, R.C. Algorithms for Skin Permeability Using Hydrogen Bond Descriptors: The Problem of Steroids. *J. Pharm. Pharmacol.* **1997**, *49*, 858–865. [CrossRef] [PubMed]
14. Abraham, M.H.; Chadha, H.S.; Mitchell, R.C. The Factors That Influence Skin Penetration of Solutes. *J. Pharm. Pharmacol.* **1995**, *47*, 8–16. [CrossRef]
15. Abraham, M.H.; Martins, F. Human Skin Permeation and Partition: General Linear Free-Energy Relationship Analyses. *J. Pharm. Sci.* **2004**, *93*, 1508–1523. [CrossRef] [PubMed]
16. Anderson, B.D.; Raykar, P.V. Solute Structure-Permeability Relationships in Human Stratum Corneum. *J. Investig. Dermatol.* **1989**, *93*, 280–286. [CrossRef] [PubMed]
17. Barratt, M.D. Quantitative Structure-Activity Relationships for Skin Permeability. *Toxicol. In Vitro* **1995**, *9*, 27–37. [CrossRef]
18. Chang, Y.-C.; Chen, C.-P.; Chen, C.-C. Predicting Skin Permeability of Chemical Substances Using a Quantitative Structure-Activity Relationship. *Procedia Eng.* **2012**, *45*, 875–879. [CrossRef]
19. Neely, B.J.; Madihally, S.V.; Robinson, R.L.; Gasem, K.A.M. Nonlinear Quantitative Structure-Property Relationship Modeling of Skin Permeation Coefficient. *J. Pharm. Sci.* **2009**, *98*, 4069–4084. [CrossRef]
20. Neumann, D.; Kohlbacher, O.; Merkwirth, C.; Lengauer, T. A Fully Computational Model for Predicting Percutaneous Drug Absorption. *J. Chem. Inf. Model.* **2006**, *46*, 424–429. [CrossRef] [PubMed]
21. Patel, H.; ten Berge, W.; Cronin, M.T.D. Quantitative Structure–Activity Relationships (QSARs) for the Prediction of Skin Permeation of Exogenous Chemicals. *Chemosphere* **2002**, *48*, 603–613. [CrossRef]
22. Potts, R.O.; Guy, R.H. A Predictive Algorithm for Skin Permeability: The Effects of Molecular Size and Hydrogen Bond Activity. *Pharm. Res.* **1995**, *12*, 1628–1633. [CrossRef] [PubMed]

23. Sobańska, A.W.; Robertson, J.; Brzezińska, E. Application of RP-18 TLC Retention Data to the Prediction of the Transdermal Absorption of Drugs. *Pharmaceuticals* **2021**, *14*, 147. [[CrossRef](#)]
24. Alonso, C.; Carrer, V.; Espinosa, S.; Zanuy, M.; Córdoba, M.; Vidal, B.; Domínguez, M.; Godessart, N.; Coderch, L.; Pont, M. Prediction of the Skin Permeability of Topical Drugs Using in Silico and in Vitro Models. *Eur. J. Pharm. Sci.* **2019**, *136*, 104945. [[CrossRef](#)] [[PubMed](#)]
25. Chen, C.-P.; Chen, C.-C.; Huang, C.-W.; Chang, Y.-C. Evaluating Molecular Properties Involved in Transport of Small Molecules in Stratum Corneum: A Quantitative Structure-Activity Relationship for Skin Permeability. *Molecules* **2018**, *23*, 911. [[CrossRef](#)] [[PubMed](#)]
26. Fitzpatrick, D.; Corish, J.; Hayes, B. Modelling Skin Permeability in Risk Assessment—The Future. *Chemosphere* **2004**, *55*, 1309–1314. [[CrossRef](#)]
27. Geinoz, S.; Guy, R.H.; Testa, B.; Carrupt, P.-A. Quantitative Structure-Permeation Relationships (QSPeRs) to Predict Skin Permeation: A Critical Evaluation. *Pharm. Res.* **2004**, *21*, 83–92. [[CrossRef](#)] [[PubMed](#)]
28. Mitragotri, S. A Theoretical Analysis of Permeation of Small Hydrophobic Solutes across the Stratum Corneum Based on Scaled Particle Theory. *J. Pharm. Sci.* **2002**, *91*, 744–752. [[CrossRef](#)] [[PubMed](#)]
29. Wilschut, A.; ten Berge, W.F.; Robinson, P.J.; McKone, T.E. Estimating Skin Permeation. The Validation of Five Mathematical Skin Permeation Models. *Chemosphere* **1995**, *30*, 1275–1296. [[CrossRef](#)]
30. Barbato, F.; Cappello, B.; Miro, A.; La Rotonda, M.; Quaglia, F. Chromatographic Indexes on Immobilized Artificial Membranes for the Prediction of Transdermal Transport of Drugs. *Il Farm.* **1998**, *53*, 655–661. [[CrossRef](#)]
31. Hidalgo-Rodríguez, M.; Soriano-Meseguer, S.; Fuguet, E.; Ràfols, C.; Rosés, M. Evaluation of the Suitability of Chromatographic Systems to Predict Human Skin Permeation of Neutral Compounds. *Eur. J. Pharm. Sci.* **2013**, *50*, 557–568. [[CrossRef](#)]
32. Jevric, L.R.; Podunavac Kuzmanovic, S.O.; Svarc Gajic, J.V.; Kovacevic, S.; Jovanovic, B.Z. RP-HPTLC Retention Data in Correlation with the In-Silico ADME Properties of a Series of s-Triazine Derivatives. *Iran. J. Pharm. Res.* **2014**, *13*, 1203–1211. [[CrossRef](#)] [[PubMed](#)]
33. Kovačević, S.; Jevrić, L.R.; Podunavac Kuzmanović, S.O.; Lončar, E.S. Prediction of In Silico ADME Properties of 1,2-O-Isopropylidene Aldohexose Derivatives. *Iran. J. Pharm. Res.* **2014**, *13*, 899–907. [[CrossRef](#)] [[PubMed](#)]
34. Lazaro, E.; Rafols, C.; Abraham, M.H.; Rosés, M. Chromatographic Estimation of Drug Disposition Properties by Means of Immobilized Artificial Membranes (IAM) and C18 Columns. *J. Med. Chem.* **2006**, *49*, 4861–4870. [[CrossRef](#)] [[PubMed](#)]
35. Martínez-Pla, J.J.; Martín-Biosca, Y.; Sagrado, S.; Villanueva-Camañas, R.M.; Medina-Hernández, M.J. Evaluation of the PH Effect of Formulations on the Skin Permeability of Drugs by Biopartitioning Micellar Chromatography. *J. Chromatogr. A* **2004**, *1047*, 255–262. [[CrossRef](#)] [[PubMed](#)]
36. Nasal, A.; Sznitowska, M.; Buciński, A.; Kaliszczan, R. Hydrophobicity Parameter from High-Performance Liquid Chromatography on an Immobilized Artificial Membrane Column and Its Relationship to Bioactivity. *J. Chromatogr. A* **1995**, *692*, 83–89. [[CrossRef](#)]
37. Soriano-Meseguer, S.; Fuguet, E.; Port, A.; Rosés, M. Estimation of Skin Permeation by Liquid Chromatography. *ADMET DMPK* **2018**, *6*, 140–152. [[CrossRef](#)]
38. Turowski, M.; Kaliszczan, R. Keratin Immobilized on Silica as a New Stationary Phase for Chromatographic Modelling of Skin Permeation. *J. Pharm. Biomed. Anal.* **1997**, *15*, 1325–1333. [[CrossRef](#)]
39. Wang, Y.; Sun, J.; Liu, H.; Liu, J.; Zhang, L.; Liu, K.; He, Z. Predicting Skin Permeability Using Liposome Electrokinetic Chromatography. *Analyst* **2009**, *134*, 267–272. [[CrossRef](#)] [[PubMed](#)]
40. Waters, L.J.; Shahzad, Y.; Stephenson, J. Modelling Skin Permeability with Micellar Liquid Chromatography. *Eur. J. Pharm. Sci.* **2013**, *50*, 335–340. [[CrossRef](#)]
41. Sobanska, A.W.; Robertson, J.; Brzezińska, E. RP-18 TLC Chromatographic and Computational Study of Skin Permeability of Steroids. *Pharmaceuticals* **2021**, *14*, 600. [[CrossRef](#)]
42. Bate-Smith, E.C.; Westall, R.G. Chromatographic Behaviour and Chemical Structure I. Some Naturally Occurring Phenolic Substances. *Biochim. Biophys. Acta* **1950**, *4*, 427–440. [[CrossRef](#)]
43. Sobańska, A.W.; Brzezińska, E. RP-18 TLC and Computational Descriptors of Skin Permeability of Sunscreens. *Skin Pharmacol. Physiol.* **2022**. [[CrossRef](#)] [[PubMed](#)]
44. Sobanska, A.W.; Brzezinska, E. Phospholipid-Based Immobilized Artificial Membrane (IAM) Chromatography: A Powerful Tool to Model Drug Distribution Processes. *Curr. Pharm. Des.* **2017**, *23*, 6784–6794. [[CrossRef](#)] [[PubMed](#)]
45. Seung, L.J. EPI Suite: A Fascinate Predictive Tool for Estimating the Fates of Organic Contaminants. *J. Bioremed. Biodegrad.* **2016**, *7*, e171. [[CrossRef](#)]
46. Sprunger, L.; Blake-Taylor, B.H.; Wairegi, A.; Acree, W.E.; Abraham, M.H. Characterization of the Retention Behavior of Organic and Pharmaceutical Drug Molecules on an Immobilized Artificial Membrane Column with the Abraham Model. *J. Chromatogr. A* **2007**, *1160*, 235–245. [[CrossRef](#)]
47. Clark, D.E. Rapid Calculation of Polar Molecular Surface Area and Its Application to the Prediction of Transport Phenomena. 2. Prediction of Blood–Brain Barrier Penetration. *J. Pharm. Sci.* **1999**, *88*, 815–821. [[CrossRef](#)] [[PubMed](#)]
48. Clark, D.E. Rapid Calculation of Polar Molecular Surface Area and Its Application to the Prediction of Transport Phenomena. 1. Prediction of Intestinal Absorption. *J. Pharm. Sci.* **1999**, *88*, 807–814. [[CrossRef](#)] [[PubMed](#)]
49. Veber, D.F.; Johnson, S.R.; Cheng, H.-Y.; Smith, B.R.; Ward, K.W.; Kopple, K.D. Molecular Properties That Influence the Oral Bioavailability of Drug Candidates. *J. Med. Chem.* **2002**, *45*, 2615–2623. [[CrossRef](#)] [[PubMed](#)]